ACS Biomaterials SCIENCE & ENGINEERING

pubs.acs.org/journal/abseba

Article

Engineered Fibrous NiTi Scaffolds with Cultured Hepatocytes for Liver Regeneration in Rats

Oleg V. Kokorev, Ekaterina S. Marchenko, Igor A. Khlusov, Alex A. Volinsky,* Yuri F. Yasenchuk, and Alexander N. Monogenov

Cite This: *ACS Biomater. Sci. Eng.* 2023, 9, 1558–1569

Read Online

ACCESS | Metrics & More | Article Recommendations

Downloaded via UNIV OF SOUTH FLORIDA on March 13, 2023 at 16:45:42 (UTC).
See https://pubs.acs.org/sharingguidelines for options on how to legitimately share published articles.

ABSTRACT: At present, the use of alternative systems to replenish the lost functions of hepatic metabolism and partial replacement of liver organ failure is relevant, due to an increase in the incidence of various liver disorders, insufficiency, and cost of organs for transplantation, as well as the high cost of using the artificial liver systems. The development of low-cost intracorporeal systems for maintaining hepatic metabolism using tissue engineering, as a bridge before liver transplantation or completely replacing liver function, deserves special attention. In vivo applications of intracorporeal fibrous nickel−titanium scaffolds (FNTSs) with cultured hepatocytes are described. Hepatocytes cultured in FNTSs are superior to their injections in terms of liver function, survival time, and recovery in a CCl_4-induced cirrhosis rats' model. 232 animals were divided into 5 groups: control, CCl_4-induced cirrhosis, CCl_4-induced cirrhosis followed by implantation of cell-free FNTSs (sham surgery), CCl_4-induced cirrhosis followed by infusion of hepatocytes (2 mL, 10^7 cells/mL), and CCl_4-induced cirrhosis followed by FNTS implantation with hepatocytes. Restoration of hepatocyte function in the FNTS implantation with the hepatocytes group was accompanied by a significant decrease in the level of aspartate aminotransferase (AsAT) in blood serum compared to the cirrhosis group. A significant decrease in the level of AsAT was noted after 15 days in the infused hepatocytes group. However, on the 30th day, the AsAT level increased and was close to the cirrhosis group due to the short-term effect after the introduction of hepatocytes without a scaffold. The changes in alanine aminotransferase (AlAT), alkaline phosphatase (AlP), total and direct bilirubin, serum protein, triacylglycerol, lactate, albumin, and lipoproteins were similar to those in AsAT. The survival time of animals was significantly longer in the FNTS implantation with hepatocytes group. The obtained results showed the scaffolds' ability to support hepatocellular metabolism. The development of hepatocytes in FNTS was studied in vivo using 12 animals using scanning electron microscopy. Hepatocytes demonstrated good adhesion to the scaffold wireframe and survival in allogeneic conditions. Mature tissue, including cellular and fibrous, filled the scaffold space by 98% in 28 days. The study shows the extent to which an implantable "auxiliary liver" compensates for the lack of liver function without replacement in rats.

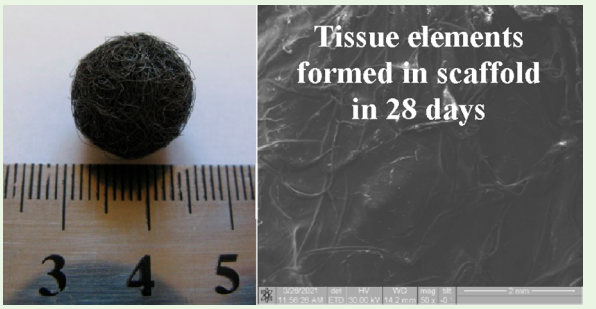

KEYWORDS: *rats, fibrous NiTi scaffold, CCl_4-induced cirrhosis, allogeneic hepatocytes, tissue engineering, regenerative therapy*

1. INTRODUCTION

According to the literature, liver disease is one of the main clinical problems, since over 600 million people suffer from liver disease worldwide. According to the World Health Organization, liver disease is the 11th leading cause of death in the world. Despite the improvement of diagnosis and treatment, accumulated risk factors and the aging of the population lead to an increase in the incidence of liver diseases. Liver transplantation is the standard for parenchymal organ transplantation and the second most common transplantation method. At the current rate of liver disease, less than 10% of the required needs are met due to a lack of liver organs.[1]

The mortality rate of patients on a waiting list in the United States is over 20%. These data do not include all patients who would require liver transplantation.[2] Given the high mortality from liver diseases, along with the rapid increase in the number of cases, there is an urgent need to develop new methods of treating liver failure. Cell therapy based on the introduction of cells and tissues is becoming an alternative to organ transplantation.

As an alternative, methods have been developed to replace liver transplantation with natural organ restoration.[3] These methods include exchange/filtration systems and hepatocyte-

Received: October 25, 2022
Accepted: February 6, 2023
Published: February 20, 2023

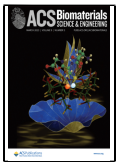

ACS Publications

© 2023 American Chemical Society

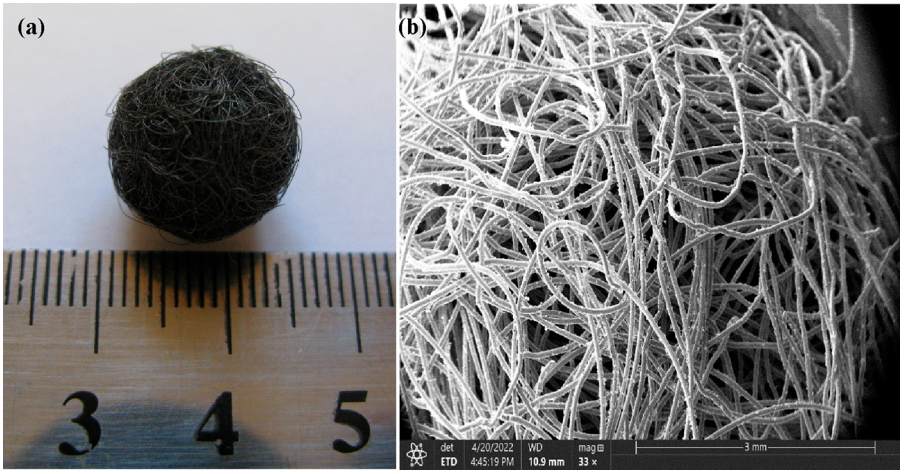

Figure 1. Fibrous nickel−titanium scaffold: (a) overall view, where the scale bar is in cm; (b) SEM image of the scaffold structure.

based exchange/filtration systems such as an extracorporeal assistive device. Their use as a bridge before liver transplantation has minimal clinical success and has a high associated cost.[4] As a result, the attention of scientists and medical doctors has turned to the development of new methods of cell and tissue therapy for the treatment and regeneration of the liver.

Cell transplantation makes it possible to overcome the acute shortage of donor organs, reduce the risk of complications associated with surgical methods of treatment, neutralize toxic effects after the use of drugs, and also prevent inhibition of the regenerative recovery of the affected organ.[5−8] The cost of cell technologies is lower compared to organ transplantation; they are safer and allow repeated transplantation several times, making a "bridge" while waiting for an organ for transplantation. They allow for providing medical care to a larger number of patients and, in some cases, allow for avoiding the use of immunosuppressive drugs. At the same time, cryobanks allow cells to be stored for a long time.[9−12]

Cell transplantation efficacy is gauged by the number of cells that will take root in the damaged tissue, the duration of their functional activity, clone development of donor cells in the recipient's body, the regenerative potential of the damaged organ, etc. Now, it is not possible to achieve high values of these parameters when injecting cells, due to the vulnerability of donor cells to the effects of the recipient's immune system.[13−15] Unlike intravascular injection, targeted cell transplantation using biomedical implants delivers a significant part of the cells into the tissue defect zone. Thus, it is urgent to search for alternative methods of introducing cellular material, which can achieve high rates of tissue and/or organ regeneration.[5,16−19]

Since the liver has excellent regenerative potential in vivo, hepatocyte cell transplantation was first proposed for the treatment of liver failure.[20] It has been shown that in a certain in vitro culture medium, liver cells can proliferate and be preserved in quantities necessary for tissue engineering. Many technologies are described in the literature: the development of specialized media, cultivation with different types of cells, the use of various growth factors that modulate the proliferative effect of hepatocytes, and the cultivation of hepatocytes in various types of three-dimensional scaffolds.[21,22] Compared to various types of cell injections, the design of implantable scaffolds is based on the immobilization of cells in three-dimensional matrices made from materials that are biocompatible with body tissues.[23,24] Various types of matrices work as a structure and biological component for hepatocytes in several contexts: they promote cell adhesion and proliferation, improve 3D integration and survival of hepatocytes in an allogeneic environment, and promote the integration of newly formed tissue into the host vasculature, thereby providing a prolonged action of the bioconstruction in the human body.[25−29]

For better support of hepatocytes and control of cellular distribution and proliferation, it is possible to control the structure of matrices: their mechanical properties, pore size and distribution, geometry, and rigidity. At the same time, biomaterials can be modified by binding them to various signaling and bioactive growth factors, controlling their release, and thus improving the functions of the hybrid liver. Progress in the study of biomaterials for tissue engineering has mainly focused on the use of scaffolds in in vitro tissue engineering of the liver. For the use of scaffolds in vivo, it is necessary to take into account the complexity and multifunctionality of the liver as an organ. In the case of in vivo applications and clinical settings, it is required to optimize scaffolds from in vitro biomaterials. The introduction of donor cells into the body in biomaterials increases their resistance to aggressive factors and survival. At the same time, the metabolism of cells in the artificial microenvironment of the scaffold can provide a decrease and/or rejection of immunosuppressants.[30−33] The main characteristics of the extracellular matrix primarily depend on the biomaterial from which it is made.[34−36] The use of numerous implantable biomaterials (natural, synthetic, ceramic, decellularized tissues, composites, etc.) as scaffolds for cells can be complicated by their carcinogenic, chemical, mechanical, antigenic, toxic, and other characteristics.[37−40]

An obstacle to the use of imported extracellular matrices in surgical practice is the fact that many of them do not have permission for clinical use in certain countries. Advantageous alternatives to the well-known analogs of extracellular matrices are nickel−titanium (NiTi, nitinol) alloys, which are biocompatible with various tissues and cells of the human body.[41−44] Their physicochemical, mechanical, and technological properties are suitable for use as biocompatible matrices for cell suspensions and prolonged vital activity of the cells immobilized in matrices.[45]

Experience using porous nickel−titanium incubators according to Gunter et al.[46] revealed their inherent disadvantages. Manufacturing methods limit the total porosity to 70%, which accordingly limits the relative volume of the contained cells'

https://doi.org/10.1021/acsbiomaterials.2c01268
ACS Biomater. Sci. Eng. 2023, 9, 1558−1569

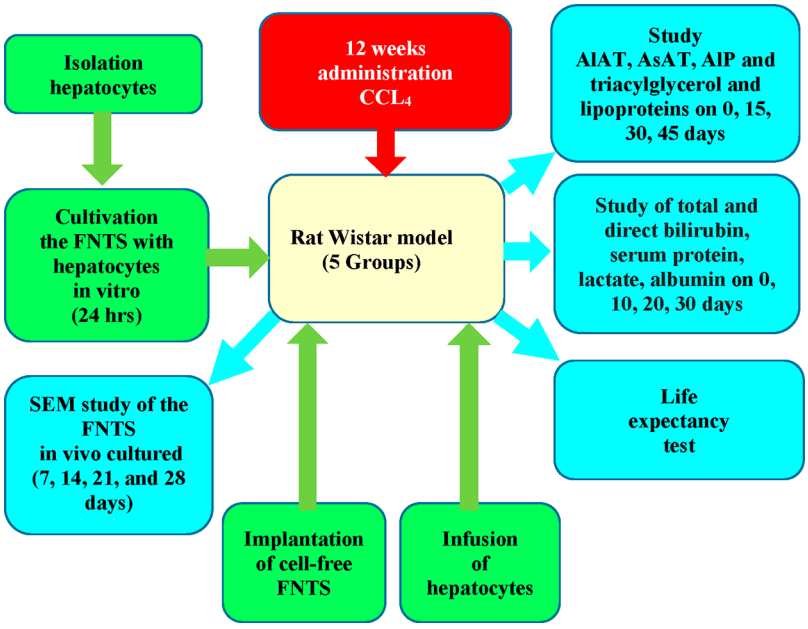

Figure 2. Schematic representation of the study design.

suspension. The bulk array of porous nickel−titanium is not completely permeable, as there are up to 3% closed pores. At the same time, nickel−titanium fibrous matrices have a porosity of more than 90%, a completely permeable structure, and depending on the density of the fibers, their mechanical properties can be controlled.[46] In this regard, the experimental study of the reparative mechanisms underlying the correction of disorders that occur in CCl_4-induced hepatitis with tissue-engineered structures from a fibrous-permeable matrix of nickel−titanium based on hepatocytes is relevant. This is a pilot study on the effectiveness of using a new fibrous matrix made from NiTi wire in maintaining the function of a liver damaged by a chemical agent.

2. MATERIALS AND METHODS

2.1. Scaffold Manufacturing. Spherical permeable fibrous scaffolds presented in Figure 1 were obtained by winding and crimping 60 μm thick nitinol wire. Wrought nitinol wire was wound to obtain a set of permeable fibrous nickel−titanium scaffolds (FNTSs) with a round shape and 15.1 ± 1.1 mm diameter, as shown in Figure 1a. The interturn distance of the scaffold in the fabricated matrices was verified using scanning electron microscopy (SEM, Quanta 200). Before saturation with cells, the scaffolds were washed in an ultrasonic bath with 70% ethanol and followed by autoclaving at 180 °C for 60 min. Until the scaffolds were saturated with cells, they were kept in the RPMI-1640 medium with 40 mg/L gentamicin. The nickel−titanium shape memory effect was not used in this experiment.

2.2. Porosity. The porosity of the scaffold was calculated using the technique described by Shimizu et al.:[47]

$$\text{porosity}\ (\%) = \frac{\text{scaffold wet weight}\ (\text{g}) - \text{scaffold dry weight}\ (\text{g})}{\text{scaffold volume}\ (\text{mm}^3)/\text{density of water}\ (\text{g/mm}^3)} \times 100\% \quad (1)$$

The 2.1 ± 0.1 mm^3 volume of the scaffolds was calculated based on its 15.1 ± 1.1 mm diameter. The dry weight of the scaffolds in grams was determined with an analytical grade scale. Scaffolds were then submerged in sterile water for 1 h and weighed to obtain their wet weight in grams. The volume of absorbed water was about 2.1 ± 0.1 mL. Here, the ± values represent the standard deviation (SD), based on 5 characterized samples.

2.3. Permeability. The fibrous matrix permeability was calculated according to the method described by Fan et al.[48] A stable hydrostatic pressure was applied to the surface of the fibrous framework. The amount of water in mL passed through the fibrous scaffold per minute was measured and used to calculate the permeability according to Darcy's law:

$$\text{permeability}\ (\mu\text{m}^3) = \frac{\text{water viscosity}\ (\text{Pa}\cdot\text{s}) \times \frac{\text{water passed through the scaffold}\ (\text{mm}^3)}{\text{min}}}{\frac{\text{cross-sectional area of the scaffold}\ (\text{mm}^2) \times \text{constant pressure}\ (\text{Pa})}{\text{scaffold length}\ (\text{mm})}} \quad (2)$$

The weight of the water that passed through the tube with the matrix per minute was measured, and the water was collected and weighed on an analytical balance. The specific gravity of water (0.997 g/cm^3) was multiplied by the weight to give the volume in mm^3. The pressure height of the water column (90 mm) was multiplied by the average cross-sectional area of the matrix (177 mm^2). The average mass flow rate of water was 10.8 g/s on average, or 650 cm^3/min volumetric flow rate.

2.4. Swelling and Water Absorption. Water swelling of the scaffold was determined as in ref 49:

$$\text{swelling ratio}\ (\%) = \frac{\text{scaffold wet weight} - \text{scaffold dry weight}}{\text{scaffold dry weight}} \times 100\% \quad (3)$$

The water uptake of the scaffold was calculated as

$$\text{water uptake}\ (\%) = \frac{\text{scaffold wet weight} - \text{scaffold dry weight}}{\text{scaffold wet weight}} \times 100\% \quad (4)$$

2.5. The Scaffold Stiffness. The scaffold stiffness was defined as the ratio of the strain ε and the stress σ independent of the scaffold size and shape. Briefly, FNTS-3D scaffolds (15 mm in diameter) were compressed four times to 10% height with 5 mm/min velocity using an Instron VNS 5969 univeral testing machine (Norwood, MA., USA). In the region of elastic linear deformation, the stiffness of the fibrous matrix[50] was calculated as

https://doi.org/10.1021/acsbiomaterials.2c01268
ACS Biomater. Sci. Eng. 2023, 9, 1558−1569

Table 1. Distribution of Laboratory Animals in the Study

experimental procedures	number of animals	sampling time
SEM imaging of hepatocytes evolution in the FNTS in vivo	n = 12	Days 7, 14, 21, and 28
Life expectancy test	4 groups, n = 5 in each group (N = 20)	N/A
Isolation of hepatocytes	n = 8	N/A
Quantitative biochemical assessment of AlAT, AsAT, AlP, and triacylglycerol and lipoproteins	5 groups, n = 20 in each group (N = 100)	Days 0, 15, 30, and 45
Quantitative assessment of total and direct bilirubin, serum protein, lactate, and albumin	5 groups, n = 20 in each group (N = 100)	Days 0, 10, 20, and 30
Total	240	

$$\text{scaffold stiffness (MPa)} = \frac{\text{applied force } (N) \times \text{initial scaffold height (mm)}}{\text{scaffold area (mm}^2) \times \text{scaffold height change (mm)}} \quad (5)$$

The mechanical properties of the NiTi wire were measured using a custom-build tensile testing apparatus designed specifically for this purpose.[51−53]

2.6. Laboratory Animals. 240 male 12−14 week old Wistar rats weighing 160−180 g were used in the experiments. Animal housing and experimental design were approved by the Bioethical Committee of Tomsk State University (approval code N20/1116/2017) and complied with international rules adopted by the European Convention for the Protection of Vertebrate Animals used for experimental and other scientific purposes, following the 2010/63/EU directive.[54] Throughout the experiments, the animals were kept in a vivarium at 20−22 °C, 50 ± 10% relative humidity in the day−night light mode. Animals were placed in standard plastic cages, 5 animals each, with small wood shavings and kept before the start of the study and during the experiments on a standard diet. In order to exclude seasonal fluctuations in the studied parameters, all experiments were carried out in the autumn−winter period. Animal euthanasia was carried out by the CO_2 overdose. The scheme of the experiments using rodents is shown in Figure 2. Groups and distribution of animals according to the written protocol by series of experiments are listed in Table 1.

2.7. Animal Tests in Vivo. CCl_4-induced cirrhosis of the liver was modeled by oral administration of a 40% oil solution of carbon tetrachloride (CCl_4) with a volume of 0.2 mL/100 g of body weight for 12 weeks once a week. Hepatocytes were isolated from the liver of Wistar rats by the modified two-step method described by Shen et al.[55] On average, 4×10^8 hepatocytes were isolated from the whole liver of an animal. For a complete experiment with injection, 8 rats were needed, listed in Table 1. The isolated hepatocytes were seeded at a final concentration of 10^7 cells/mL in FNTS and cultured in vitro at 37 °C, 5% CO_2, and 100% humidity for 24 h.

After the administration of ketamine (50 mg/kg intramuscularly), the rats were fixed on the operating table with adhesive tape in the supine position. The skin was shaved, dried with gauze, and disinfected with a 1.5% betadine solution. The operation area was protected with a sterile drape. Subcutaneous tissue and skin of the abdominal wall were cut at 2−3 cm along the midline. The scaffolds were implanted into the abdominal cavity and placed on the anterior surface of the liver, followed by continuous absorbable suture application. After the operation, the rats were returned to individual cages, and after 3 h, they were put together, five rats per cage.

Rats were divided into 5 groups:

- Intact rats (Control)
- Rats with CCl_4-induced cirrhosis (CCl_4)
- Rats with cirrhosis-induced administration of CCl_4 followed by implantation of acellular FNTSs (sham-operated group, CCl_4+NiTi)
- Rats with cirrhosis of hepatitis-induced administration of CCl_4 and subsequent infusion of 2 mL of hepatocytes (10^7 cells/mL; CCl_4+Cells)
- Rats with cirrhosis caused by CCl_4 administration and subsequent implantation of FNTSs cultured in vitro with hepatocytes (10^7 cells/mL; CCl_4+NiTi+Cells)

The groups are described in the paper in detail. We considered the group with fibrous matrix implantation with hepatocytes as an experimental group. At the same time, the control group for it was the group with the injection of hepatocytes. Also, the control group included a group with surgical intervention in the form of implantation of a fibrous structure without cells (the effect of the operation on the studied parameters). To understand the effectiveness of the effects of hepatocytes on the restoration of liver function, a group was introduced with an experimental model of liver failure without any manipulations. The control group without modeling liver failure was introduced to control the created model of liver failure and to control the improvement of parameters (approaching biochemical parameters to the norm (indicators of healthy animals)).

2.8. Biochemical Evaluation Methods. Serum and plasma were taken from peripheral blood, and the concentrations of aspartate aminotransferase (AsAT), alanine aminotransferase (AlAT), alkaline phosphatase (AlP), triacylglycerol, and lipoproteins were assessed on days 0, 15, 30, and 45 and total and direct bilirubin, serum protein, lactate, and albumin, on days 0, 10, 20, and 30 using a Beckman Coulter AU480 biochemical analyzer with standard Beckman Coulter reagents (USA).

2.9. SEM Study. SEM of tissue engineering extracts from rats was carried out using Quanta 200 3D SEM (FEI Co., Japan) at a voltage of 30 kV on the 7th, 14th, 21st, and 28th days after implantation. FTNS was washed with PBS and fixed with diluted 2.5% glutaraldehyde solution for 1 h and then washed three times with PBS for 15 min and fixed in 1% solution of OsO_4 (Sigma-Aldrich) for 1 h and washed three times with PBS for 15 min. After dehydration in alcohols of increasing concentrations (25%, 50%, 70%, 90%, and 100% ethanol), the FTNSs were kept in each solution for 15 min, then dried, and observed in SEM.

2.10. Statistical Analysis. The obtained results were processed using Statistica 10.0 software (StatSoft, Inc., USA). The results are presented in the form of the average value ± SD. Measurements from 5 animals were used for each data point. Error bars in all figures represent standard deviation. If the distribution of the results was not normal, the reliability of differences in the studied characteristics between groups was tested using the nonparametric Mann−Whitney U test. Differences between experimental groups were analyzed with $p \leq 0.05$ considered statistically significant.

3. RESULTS

3.1. Fibrous Nickel−Titanium Scaffold (FNTS). Scaffold properties are summarized in Table 2. Pore sizes can be varied by the density of winding threads in a given scaffold. The scaffolds were produced using the same winding method, so the pore size distribution was similar between the scaffolds.

Table 2. Characteristics of FNTS Scaffolds

FNTS scaffolds	porosity, %	permeability, μm^2	water uptake, %	swelling ratio, %
Average	91.1	62.8	70	232
Standard Deviation	2.4	2.6	1.7	12.4

The porosity of the matrices, measured five times, was approximately 91.1 ± 2.4%, together with a high permeability of 62.8 ± 2.6 μm^2, which was measured from five different matrices (3 times for each matrix). This indicates a complete lack of

https://doi.org/10.1021/acsbiomaterials.2c01268
ACS Biomater. Sci. Eng. 2023, 9, 1558−1569

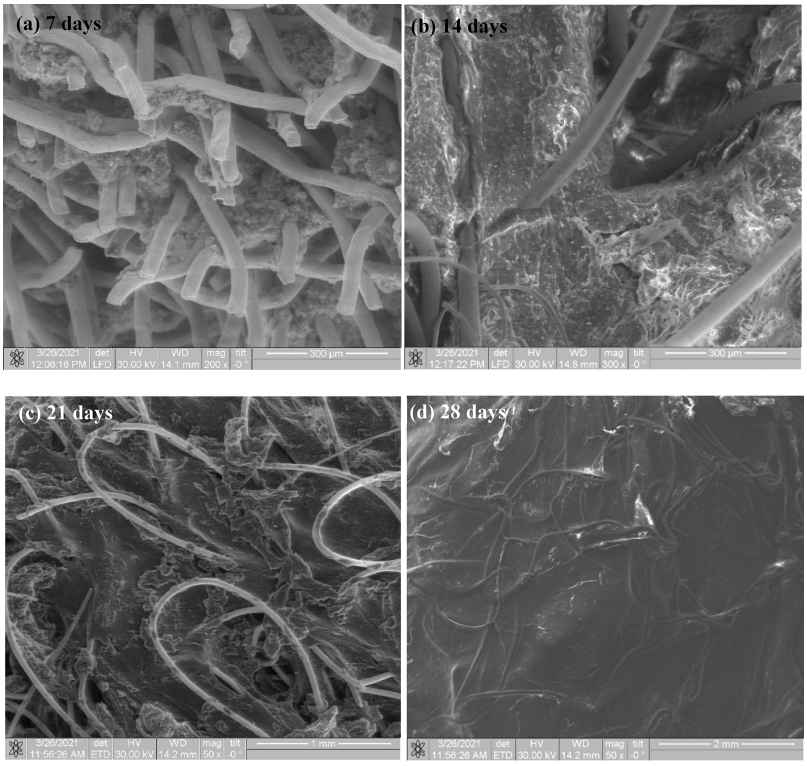

Figure 3. SEM images of FTNS sections on (a) day 7, (b) day 14, (c) day 21, and (d) day 28 after implantation.

closed poses in the scaffold. The swelling coefficient was 232 ± 12.4%. Water absorption of 70 ± 1.7% indicates the high hydrophilicity of the framework. Here, the ± values represent the standard deviation. The dry FNTS 3D matrix has a stiffness of about 7.8 kPa, which is comparable to the stiffness of healthy human liver tissue.[55] Pore sizes can be varied by the density of winding threads in a given scaffold. The scaffolds were produced using the same winding method, so the pore size distribution was similar between the scaffolds.

This fibrous scaffold has the following advantages compared to porous structures. There is full permeability of water-based suspensions since porous structures have limited permeability due to the presence of closed pores and small pores into which cells do not enter. Filling porous spaces with the same density of cells of large volumes of more than 3 mm^3 is possible only by stimulated methods under pressure. The hydrophilicity and elasticity of titanium nickelide threads make it possible to fill the entire volume of empty space in a given scaffold with the same cell density. In our experience, compared with porous NiTi made by self-propagating high-temperature synthesis, there should be no closed pores, which is important for tissue growth in a biologically relevant sense. Another important parameter is the scaffold stiffness, which is comparable to the stiffness of healthy liver tissue.

3.2. SEM Characterization. SEM was used to observe the postimplantation evolution of hepatocytes within the FNTSs in 7-day intervals for 28 days. Good adhesion of hepatocytes and tissue growth within the pores was observed. Figure 3a shows multiple integrations of cell groups within the pores after 7 days past implantation of the scaffold in experimental animals. After implantation on day 14, SEM images of FNTSs show cell multiplication with increased cell population in the fibrous scaffold pores, forming tissue elements. Figure 3c,d shows the final stages of complete filling of the pores in the fibrous structure on days 21 and 28.

3.3. Biochemical Analysis. During 45 days, the change in the concentration of hepatic enzymes in the blood serum of animals was measured: aspartate aminotransferase (AsAT), alanine aminotransferase (AlAT), alkaline phosphatase (AlP), triacylglycerol, and lipoproteins. As known from the literature, the development of CCl_4-induced cirrhosis is accompanied by necrosis, localized centrilobular, and degeneration of hepatocytes and, subsequently, of the entire liver.[56] In our studies, these changes were observed in connection with an increase in transaminase enzymes: AsAT, AlAT, and AlP (Figures 4–6).

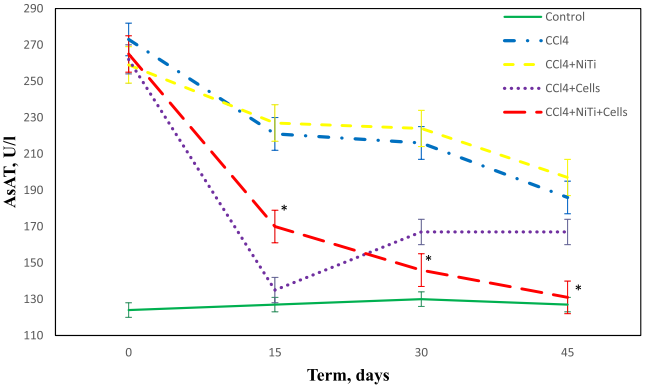

Figure 4. AsAT (U/L) development during a 45-day observation period in Wistar rats with CCl_4-induced cirrhosis. Each data point is represented by an average value and standard deviation, based on measurements from 5 animals [*: Statistically significant difference between the CCl_4+NiTi+Cells and CCl_4, CCl_4+NiTi, and CCl_4+Cells groups ($p < 0.05$)].

https://doi.org/10.1021/acsbiomaterials.2c01268
ACS Biomater. Sci. Eng. 2023, 9, 1558−1569

Blood serum taken a day after the end of carbon tetrachloride administration showed a significant increase level of the enzyme aspartate transferase from 124 U/L to 273 U/L (2.2 times), which indicated the toxic effect of carbon tetrachloride on the liver, causing hepatocyte damage. In the group where the liver cells were implanted by injection, there was a rapid decrease in the concentration of this enzyme on the 15th day after the injection, but on the 30th day, there was an increase in this enzyme, showing a short-term effect of the injected liver cells. In group CCl_4+NiTi+Cells, aspartate transferase activity gradually decreased throughout the study period, amounting to 131 U/L on the 45th terminal day of the study, which is comparable with the control group in Figure 4.

The indicators of biochemical analyses of blood serum taken 1 day after the end of the introduction of carbon tetrachloride showed a statistically significant increase in the level of the enzyme alanine transferase (AlAT), from 51 U/L to 96 U/L (1.9 times), which indicated the destruction of liver cells (cytolysis) caused by CCl_4 toxic effects on the liver. In the group where liver cells were implanted by injection, there was a rapid decrease in the concentration of the AlAT enzyme on the 15th day, but later (on the 30th and 45th days), there was an increase in its concentration to the level of CCl_4 and control groups. In the CCl_4+NiTi+Cells group at the same time, the activity of alanine transferase steadily decreased throughout the study period, reaching 57 U/L on the 45th day of the study in Figure 5.

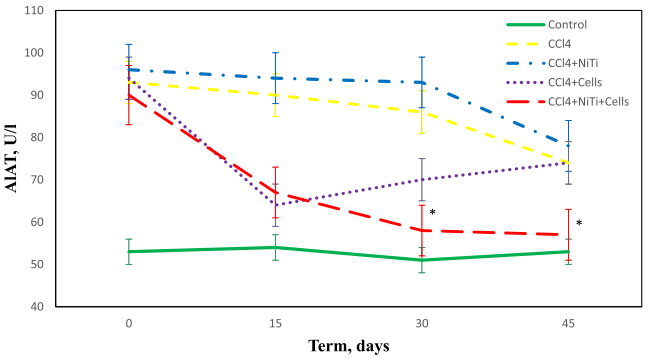

Figure 5. AlAT (U/L) development during a 45-day observation period in Wistar rats with CCl_4-induced cirrhosis. Each data point is represented by an average value and standard deviation, based on measurements from 5 animals [*: Statistically significant difference between the CCl_4+NiTi+Cells and CCl_4, CCl_4+NiTi, and CCl_4+Cells groups ($p < 0.05$)].

Blood tests taken 1 day after the end of the introduction of CCl_4 showed a significant increase in the level of the enzyme alkaline phosphatase, from 158 U/L to 285 U/L (1.8 times), indicating significant damage to the enzymatic apparatus of the liver after the introduction of carbon tetrachloride in Figure 6. In another group, where liver cells were implanted by injection, on the 15th day after the injection, a rapid decrease in the concentration of this enzyme was observed, although on the 45th day, a significant increase in the enzyme was noted, compared with the CCl_4-induced cirrhosis followed by FNTS implantation with the hepatocytes group (CCl_4+NiTi+Cells), which indicated a short-term effect of the injected liver cells. Alkaline phosphatase levels in this group consistently decreased throughout the study period, decreasing to healthy intact animals, 171 U/L on the 45th day of the study in Figure 6.

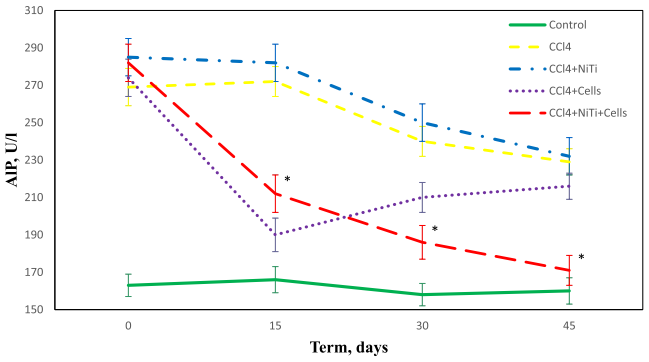

Figure 6. AlP (U/L) development during a 45-day observation period in Wistar rats with CCl_4-induced cirrhosis. Each data point is represented by an average value and standard deviation, based on measurements from 5 animals [*: Statistically significant difference between the CCl_4+NiTi+Cells and CCl_4, CCl_4+NiTi, and CCl_4+Cells groups ($p < 0.05$)].

The study of the CCl_4-induced liver failure dynamics made it possible to establish that, on the first day after modeling liver failure, the total blood serum protein sharply decreased from 75 g/L to 47 g/L (1.6 times in Figure 7) and the level of liver

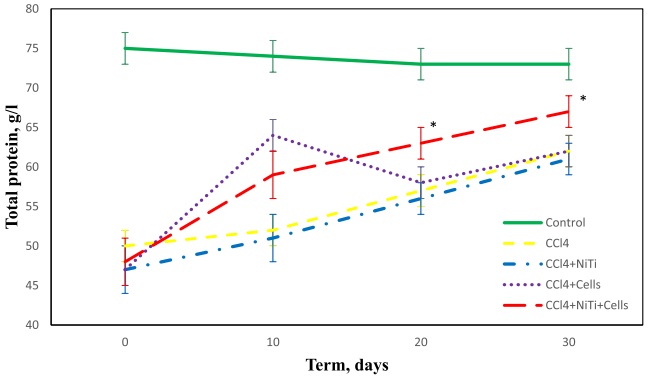

Figure 7. Comparative test of total serum protein test during a 30-day observation period in Wistar rats with CCl_4-induced cirrhosis. Each data point is represented by an average value and standard deviation, based on measurements from 5 animals [*: Statistically significant difference between the CCl_4+NiTi+Cells and CCl_4, CCl_4+NiTi, and CCl_4+Cells groups ($p < 0.05$)].

enzymes increased sharply in Figures 4−6. Surgical implantation of fibrous nickel−titanium scaffolds without cells did not cause significant fluctuations in the recorded parameters in experimental animals. Only small shifts in the studied parameters were noted, which did not lead to reliably significant results. The introduction of liver cells by injection led to a significant increase in total serum protein up to 64 g/L on the 10th day of the study in Figure 7. These data correlate with changes in the level of cytolytic enzymes described earlier. On the 30th day, there was a rapid decrease in the concentration of serum protein in the CCl_4-induced cirrhosis followed by FNTS implantation with the hepatocytes group (CCl_4+NiTi+Cells) and a gradual return to normal on the 45th day of the experiment.

The level of total albumin in Figure 8 sharply decreased after the course administration of carbon tetrachloride in all groups with model liver failure from 31 g/L to 12 g/L (by 2.6 times). At the same time, in the group of sham-operated animals, this indicator did not have significant differences from the

https://doi.org/10.1021/acsbiomaterials.2c01268
ACS Biomater. Sci. Eng. 2023, 9, 1558−1569

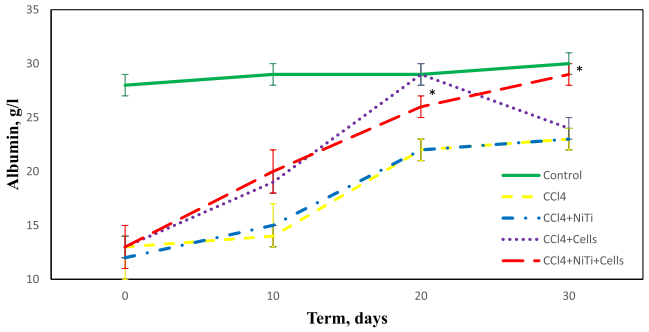

Figure 8. Change of serum albumin concentration during a 30-day observation period in Wistar rats with CCl_4-induced cirrhosis. Each data point is represented by an average value and standard deviation, based on measurements from 5 animals [*: Statistically significant difference between the CCl_4+NiTi+Cells and CCl_4, CCl_4+NiTi, and CCl_4+Cells groups ($p < 0.05$)].

corresponding control group. In the group with injected liver cells, a significant increase in this indicator was observed only on the 10th and 20th days compared with control groups, and a significant decrease in this indicator on the 30th day compared with the experimental group indicates the short duration of this effect ($p < 0.05$ compared to the CCl_4+NiTi+Cells group). The increase in albumin levels was observed constantly in the experimental group throughout the entire period of the study, reaching a maximum on the 30th day of the study of 30 g/L in Figure 8.

The study of CCl_4-induced liver failure development made it possible to establish that, on the first day after modeling liver failure, acidosis began to increase (the concentration of lactic acid increased from 1.5 mmol/L to 4.4 mmol/L in Figure 9), and

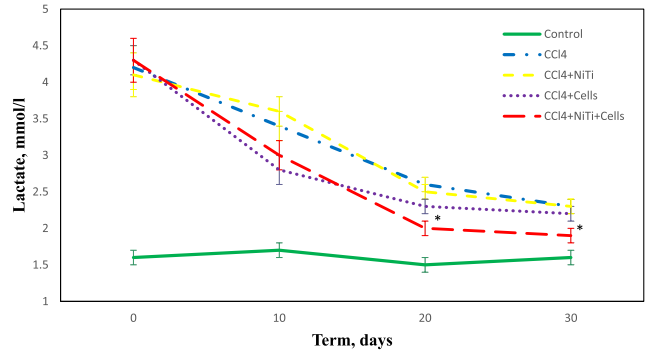

Figure 9. Comparative dynamics changes of lactate (lactic acid) concentration during a 30-day observation period in Wistar rats with CCl_4-induced cirrhosis. Each data point is represented by an average value and standard deviation, based on measurements from 5 animals [*: Statistically significant difference between the CCl_4+NiTi+Cells and CCl_4, CCl_4+NiTi, and CCl_4+Cells groups ($p < 0.05$)].

the level of hepatic enzymes sharply increased in Figures 4–6. Surgical implantation of FNTSs without cells did not cause significant fluctuations in the recorded parameters in experimental animals. Only small shifts in the studied parameters were noted, which did not lead to reliably significant results. The introduction of liver cells by injection led to a significant increase in total serum protein to 58 g/L in Figure 7 and a decrease in serum acidosis, which shows a decrease in lactate to 2.9 mmol/L in Figure 9. On the 20th day, there was a rapid decrease in the concentration of lactate in this group and a gradual return to normal on the 30th day of the CCl_4+NiTi+Cells group.

We associate the decrease in concentration with the short-term action of the cells that were introduced into the suspension; their functionality quickly degrades under the influence of immune factors, the allogeneic organism.

Massive destruction of hepatocytes under the action of carbon tetrachloride naturally led to a significant increase in the levels of bilirubin (total by 4.7 times; direct by 7.1 times) and triacylglycerides (by 3.6 times) and a small increase and decrease of high-density lipoprotein, respectively (by 2.1 times and by 2 times), in the blood plasma of pathological control rats compared to intact control. Implantation of FNTS populated by allogeneic liver cells also smoothed out a sharp increase in bilirubin after the course administration of carbon tetrachloride, where the bilirubin concentration reached 3.2 μmol/L. Bilirubin concentration smoothly decreased and on the 30th day reached 2.4 μmol/L, which was not observed in the group with injected cells ($p \leq 0.05$ compared with the CCl_4+Cells group in Figure 10).

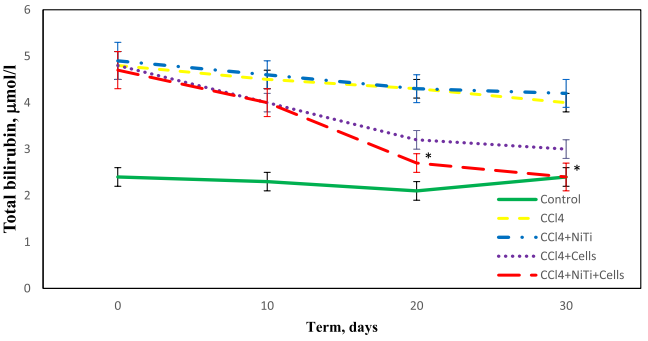

Figure 10. Change of serum total bilirubin concentration during a 30-day observation period in Wistar rats with CCl_4-induced cirrhosis. Each data point is represented by an average value and standard deviation, based on measurements from 5 animals [*: Statistically significant difference between the CCl_4+NiTi+Cells and CCl_4, CCl_4+NiTi, and CCl_4+Cells groups ($p < 0.05$)].

On the first day after the course introduction of carbon tetrachloride, there was an increase in the direct bilirubin content (4.19 ± 0.6 μmol/L in Figure 11), indicating a decrease

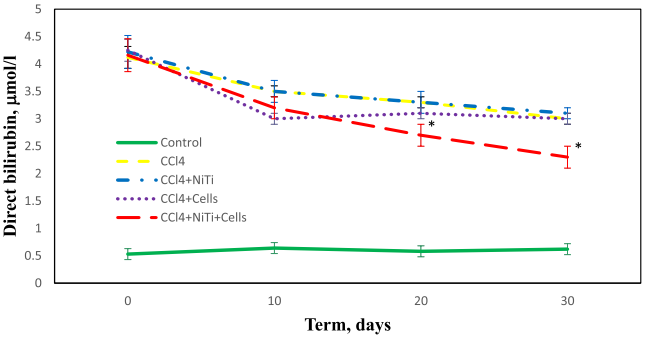

Figure 11. Comparative test of serum direct bilirubin concentration during a 30-day observation period in Wistar rats with CCl_4-induced cirrhosis. Each data point is represented by an average value and standard deviation, based on measurements from 5 animals [*: Statistically significant difference between the CCl_4+NiTi+Cells and CCl_4, CCl_4+NiTi, and CCl_4+Cells groups ($p < 0.05$)].

https://doi.org/10.1021/acsbiomaterials.2c01268
ACS Biomater. Sci. Eng. 2023, 9, 1558–1569

in the disposal function of the liver. The content of direct bilirubin after transplantation of liver cells on the extracellular matrix of nickel−titanium normalized and approached the initial level on the 30th day after the course introduction of carbon tetrachloride. However, in the control group, these parameters did not reach the absolute values of the intact animals after the introduction of carbon tetrachloride.

The destruction of hepatocytes under the action of carbon tetrachloride shows a significant increase in the level of triacylglycerides (1.75 ± 0.06 μmol/L; by 3.6 times) in the plasma of pathological control rats compared to intact control rats in Figure 12. In this regard, in our proposed approach to

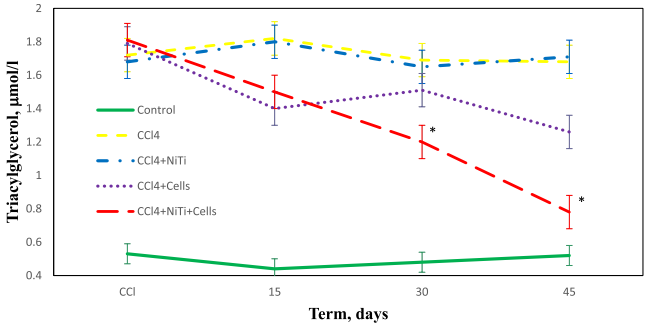

Figure 12. Comparative dynamics of triacylglycerol concentration in the blood serum during a 45-day observation period in Wistar rats with CCl_4-induced cirrhosis. Each data point is represented by an average value and standard deviation, based on measurements from 5 animals [*: Statistically significant difference between the CCl_4+NiTi+Cells and CCl_4, CCl_4+NiTi, and CCl_4+Cells groups ($p < 0.05$)].

therapy with injection, the introduction of cells significantly reduced the level of triacylglycerides on the 30th day. At the same time, the introduction of hepatocytes into FNTSs significantly reduced the level of triacylglycerides in Figure 12.

When modeling liver failure using carbon tetrachloride, an imbalance in the lipoprotein system occurred; this is how a significant decrease in high-density lipoproteins and an increase in low-density lipoproteins occurred (Figures 13 and 14). In rats with experimental liver cirrhosis, the result of cell therapy with scaffolds was a significantly low level of low-density lipoproteins at 30 and 45 days of the study than in the pathological control; in

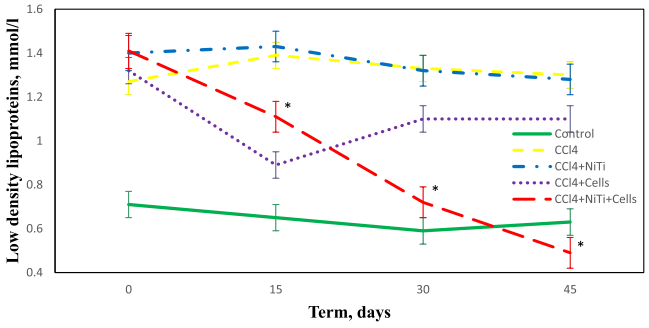

Figure 13. Change of low-density lipoprotein concentration during a 45-day observation period in Wistar rats with CCl_4-induced cirrhosis. Each data point is represented by an average value and standard deviation, based on measurements from 5 animals [*: Statistically significant difference between the CCl_4+NiTi+Cells and CCl_4, CCl_4+NiTi, and CCl_4+Cells groups ($p < 0.05$)].

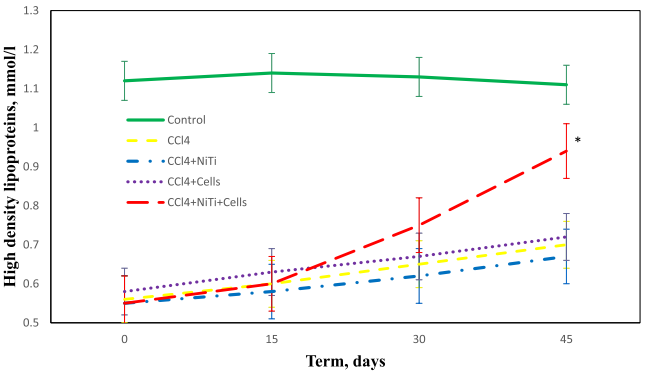

Figure 14. Comparative dynamics of high-density lipoproteins concentration in the blood serum during a 45-day observation period in Wistar rats with CCl_4-induced cirrhosis. Each data point is represented by an average value and standard deviation, based on measurements from 5 animals [*: Statistically significant difference between the CCl_4+NiTi+Cells and CCl_4, CCl_4+NiTi, and CCl_4+Cells groups ($p < 0.05$)].

contrast, the concentration of high-density lipoproteins increased insignificantly at 30 and 45 days in Figure 14.

The positive effects of cells implanted on a fibrous scaffold were significantly higher in relation to serum parameters of lipid metabolism. Thus, the introduction of cells into FNTS significantly reduced low-density lipoproteins at all points of the study in relation to the pathological control and increased high-density lipoproteins at the terminal point of the study in Figure 14.

Thus, the course introduction of carbon tetrachloride causes the development of cirrhosis of the liver. Violation of the structure of the liver (necrosis of hepatocytes) is accompanied by a violation of its synthetic function, which is shown by the results of a study of serum enzymes and indicators of carbohydrate and lipid metabolism. In liver cirrhosis, the positive effects of cells injected without FNTSs in relation to serum parameters were inferior to those with the introduction of cells into FNTSs.

The data of this study indicate that the implantation of FNTSs populated with liver cells in rats with modeled liver failure leads to an improvement in hepatospecific blood parameters and biochemical parameters. An analysis of the changes in biochemical parameters showed their improvement after the injection of liver cells into the peritoneal cavity of animals with experimental hepatitis, but the effect was short-lived.

3.4. Animal Life Expectancy. The life span of animals left to survive also confirmed the significance of the use of fibrous scaffolds for the correction of liver failure in the experiment. The formation of a hepatotoxic model of hepatitis led to early mortality of animals, where the main mortality range was from 79 to 118 days after the CCl_4 injection cycle in Table 3. It was noted that the life expectancy in the group with the introduction of carbon tetrachloride was 97 ± 15 days. In the group of sham-operated animals with intact FNTS implantation, life expectancy was unreliably reduced and amounted to 87 ± 16 days.

In the group where liver cells were injected, life expectancy increased by 1.5 times and amounted to 148 ± 16 days. Nickel−titanium permeable fibrous scaffolds with immobilized liver cells proved to be the most effective in the group where the life expectancy turned out to be a maximum of 238 ± 24 days, which exceeded the control with carbon tetrachloride by 2.5 times and

https://doi.org/10.1021/acsbiomaterials.2c01268
ACS Biomater. Sci. Eng. 2023, 9, 1558−1569

Table 3. Life Expectancy of Wistar Rats with CCl_4-Induced Cirrhosis in the Experimental Groups[a]

	lifespan, days					
experimental group	1st rat	2nd rat	3rd rat	4th rat	5th rat	average ± SD
CCl_4	79	88	95	104	118	97 ± 15
CCl_4+NiTi	69	72	91	93	109	87 ± 16
CCl_4+Cells	124	141	149	156	169	148 ± 16
CCl_4+NiTi+Cells	207	227	235	248	272	238 ± 24

[a]Here, the ± values represent the standard deviation.

the group with injected liver cells by 1.6 times, Table 3. Here, the ± values represent the standard deviation.

The results of this research indicate that the implantation of extracellular matrices inhabited by liver cells in animals with chemically induced liver cirrhosis leads to a decrease in animal mortality. Found differences in CCl_4+Cells and CCl_4+NiTi +Cells groups presumably associated with faster elimination of isolated allogeneic hepatocytes in the injection group due to their rapid elimination by immune rejection factors. A typical situation also arises in clinical conditions with the introduction of isolated liver cells; therefore, to increase the therapeutic corrective effect of liver cells in liver failure, additional infusions of a suspension of these cells are carried out in patients[57] with the aim of prolonged regenerative processes in the recipient's liver.

Differences between these two groups CCl_4 and CCl_4+NiTi in life expectancy are not significant. However, a surgical intervention performed during the implantation of the fibrous matrix has some effect on the reduction of life expectancy. This control group was introduced to exclude the effect of surgery on the model of liver failure.

4. DISCUSSION

For successful liver regeneration, cells that make up this tissue are needed, contributing to the complete restoration of the organ. Despite liver transplantation as the main method of treatment for liver failure, hepatocytes are the only cells for in vitro liver cellular therapy. Transplantation of allogenic mature hepatocytes or liver tissue engineering in vivo has been investigated and described in some papers.[56−59] The spatial configuration of FNTSs is favorable for the attachment and reproduction of isolated hepatocytes, synthesis of extracellular matrix, and formation of functional liver tissue.

The main advantages of this scaffold are biocompatibility of the nickel−titanium wire from which the scaffold is made, large free volume, permeability, and porous surface of the threads favorable for cell adhesion. The topology of fibrous NiTi scaffolds has been previously identified and studied in some tissue systems, where these factors have been partially investigated and confirmed, while the main characteristics of the material of fibrous samples vary insignificantly.[60−62] When chemical agents damage structural liver cells, such as carbon tetrachloride, a link of stem cells is normally activated, which restores cells that have lost their functions. However, for several reasons, including aging, large doses of damaging agents, and chronically acting factors, stem cells are not able to provide physiological protection for damaged cells.

With substitution therapy by injecting functionally active allogeneic cells, a partial and short-term correction of the functional failure of organs and tissues in case of their damage is achieved. In this case, the transplanted cells take on the function of damaged cells, restoring organ failure. At the same time, allogeneic cells undergo rapid destruction upon direct contact with host immunity factors and quickly lose their functional ability.[1,6]

The biocompatible nickel−titanium scaffold allows the transplanted cells to attach to the wire scaffold and function, forming a young tissue structurally similar to the mother's organ. The prolonged functioning of cells shown in this paper due to the protective function of the scaffold leads to more effective therapeutic results and an increase in the lifespan of experimental animals.

Thus, our research on the viability of liver cells in implantable fibrous scaffolds made of nickel−titanium showed their suitability for creating autonomously functioning liver units. The viability of cell populations in a nickel−titanium scaffold is ensured not only by the high saturation of the scaffold with cells but also by the creation of favorable conditions, including permeability that facilitates the delivery of oxygen and nutrients, to create stable tissue-like structures and their long-term autonomous functioning. The biocompatibility of fibrous nickel−titanium scaffolds was studied, and a regenerative effect was found after their implantation in CCl_4-induced hepatitis. The obtained data sufficiently proved the efficacy and safety of the use of permeable fibrous nickel−titanium scaffolds in laboratory animals.

5. CONCLUSIONS

This pilot study used permeable fibrous nickel−titanium scaffolds to demonstrate their effectiveness in maintaining damaged liver in rats. It is believed that the creation of intracorporeal autonomous constructions of the "auxiliary liver" based on permeable fibrous nickel−titanium scaffolds can be widely used for the treatment of liver failure. The proposed design

- eliminates the need to use complex perfusion systems and complex abdominal operations;
- allows the use of a transplantable 3D wireframe made of nickel−titanium wire to create conditions for the adhesion and reproduction of liver cells that form a tissue-like structure;
- allows the creation of adequate conditions for the diffusion of oxygenated interstitial fluid and germination of tissues and blood vessels and provides optimal conditions for the vital activity of immobilized liver cells;
- involves the use of both autologous cells, which reduce immune activation, and allogeneic liver cells, which can allow a transplanted tissue-engineered construct to have a long-term bioregulatory organ-specific effect on the liver and body without the use of immunosuppressants.

The effectiveness of the use of implantable intracorporeal autonomous structures of the "auxiliary liver" based on nickel−titanium, approved for use in medicine, and the relatively low

https://doi.org/10.1021/acsbiomaterials.2c01268
ACS Biomater. Sci. Eng. 2023, 9, 1558−1569

cost of its use should contribute to the introduction of a new method of treating liver failure in clinical practice.

■ ASSOCIATED CONTENT

Data Availability Statement

The raw/processed data required to reproduce these findings cannot be shared at this time as the data also forms part of an ongoing study.

■ AUTHOR INFORMATION

Corresponding Author

Alex A. Volinsky − *National Research Tomsk State University, Tomsk 634050, Russia; Department of Mechanical Engineering, University of South Florida, Tampa, Florida 33620, United States;* orcid.org/0000-0002-8520-6248; Email: volinsky@usf.edu

Authors

Oleg V. Kokorev − *National Research Tomsk State University, Tomsk 634050, Russia; Siberian State Medical University, Tomsk 634050, Russia*

Ekaterina S. Marchenko − *National Research Tomsk State University, Tomsk 634050, Russia*

Igor A. Khlusov − *Siberian State Medical University, Tomsk 634050, Russia;* orcid.org/0000-0003-3465-8452

Yuri F. Yasenchuk − *National Research Tomsk State University, Tomsk 634050, Russia*

Alexander N. Monogenov − *National Research Tomsk State University, Tomsk 634050, Russia*

Complete contact information is available at: https://pubs.acs.org/10.1021/acsbiomaterials.2c01268

Notes

The authors declare no competing financial interest.

■ ACKNOWLEDGMENTS

This research was supported by the Mega grant from the Government of the Russian Federation No. 220 of 09 April 2010 (Agreement No. 075-15-2021-612 of 04 June 2021).

■ REFERENCES

(1) Bram, Y.; Nguyen, D.-T.; Gupta, V.; Park, J.; Richardson, C.; Chandar, V.; Schwartz, R. E. Annual Review of Biomedical Engineering Cell and Tissue Therapy for the Treatment of Chronic Liver Disease. *Annu. Rev. Biomed. Eng.* **2021**, *23*, 517−46.

(2) Dienstag, J. L.; Cosimi, A. B. Liver transplantation—a vision realized. *N. Engl. J. Med.* **2012**, *367*, 1483−85.

(3) Kandiah, P. A.; Subramanian, R. M. Extracorporeal devices. *Crit. Care Clin.* **2019**, *35*, 135−150.

(4) Lee, K. C.; Stadlbauer, V.; Jalan, R. Extracorporeal liver support devices for listed patients. *Liver Transpl.* **2016**, *22*, 839−48.

(5) Litvinova, E. S.; Konoplya, N. N.; Shulginova, A. A.; Kharchenko, A. V. Proteins of allogeneic hepatocytes and pharmacological preparations for the correction of immunometabolic disorders in experimental liver pathology. *Research Results in Pharmacology* **2021**, *7* (2), 83−99.

(6) Tatsumi, K.; Okano, T. Hepatocyte Transplantation: Cell Sheet Technology for Liver Cell Transplantation. *Curr. Transpl. Rep.* **2017**, *4*, 184−192.

(7) Giordano, A.; Galderisi, U.; Marino, I. R. From the Laboratory Bench to the Patient's Bedside: An Update on Clinical Trials With Mesenchymal Stem Cells. *J. Cell. Physiol.* **2007**, *211*, 27−35.

(8) Huang, Y.; Miyamoto, D.; Hidaka, M.; Adachi, T.; Gu, W.-L.; Eguchi, S. Regenerative medicine for the hepatobiliary system: A review. *J. Hepatobiliary Pancreat. Sci.* **2021**, *28*, 913−930.

(9) Mirdamadi, E. S.; Kalhori, D.; Zakeri, N.; Azarpira, N.; Solati-Hashjin, M. Liver Tissue Engineering as an Emerging Alternative for Liver Disease Treatment. *Tissue Engineering: Part B* **2020**, *26* (2), 145−163.

(10) Yang, H.; Sun, L.; Pang, Y.; Hu, D.; Xu, H.; Mao, S.; Peng, W.; Wang, Y.; Xu, Y.; Zheng, Y.; Du, S.; Zhao, H.; Chi, T.; Lu, X.; Sang, X.; Zhong, S.; Wang, X.; Zhang, H.; Huang, P.; Sun, W.; Mao, Y. Three-dimensional bioprinted hepatorganoids prolong survival of mice with liver failure. *Gut.* **2021**, *70*, 567−574.

(11) Reznik, O. N.; Kuzmin, D. O.; Reznik, A. O. Biobanks as the Basis for Developing Biomedicine: Problems and Prospects. *Mol. Biol.* **2017**, *51* (5), 666−673.

(12) Manning Fox, J. E.; Lyon, J.; Dai, X. Q.; Wright, R. C.; Hayward, J.; van de Bunt, M.; Kin, T.; Shapiro, A. M. J.; McCarthy, M. I.; Gloyn, A. L.; Ungrin, M. D.; Lakey, J. R.; Kneteman, N. M.; Warnock, G. L.; Korbutt, G. S.; Rajotte, R. V.; MacDonald, P. E. Human islet function following 20 years of cryogenic biobanking. *Diabetologia* **2015**, *58*, 1503−1512.

(13) Yang, L.; Chueng, Sy-T; Li, Y.; Patel, M.; Rathnam, C.; Dey, G.; Wang, L.; Cai, L.; Lee, K.-B. A biodegradable hybrid inorganic nanoscaffold for advanced stem cell therapy. *Nature Communication* **2018**, *9*, 3147.

(14) Mardones, R.; Jofré, C. M.; Minguell, J. J. Cell Therapy and Tissue Engineering Approaches for Cartilage Repair and/or Regeneration. *International Journal of Stem Cells* **2015**, *8*, 48−53.

(15) Sabetkish, S.; Kajbafzadeh, A.-M.; Sabetkish, N.; Khorramirouz, R.; Akbarzadeh, A.; Seyedian, S. L.; Pasalar, P.; Orangian, S.; Beigi, R. S.; Aryan, Z.; Akbari, H.; Tavangar, S. M. Whole-organ tissue engineering: Decellularization and recellularization of three-dimensional matrix liver scaffolds. *Wiley Periodicals, Inc. J. Biomed. Mater. Res. Part A* **2015**, *103A*, 1498−1508.

(16) Matsuura, K.; Utoh, R.; Nagase, K.; Okano, T. Cell sheet approach for tissue engineering and regenerative medicine. *J. Controlled Release* **2014**, *190*, 228−239.

(17) Iansante, V.; Mitry, R. R.; Filippi, C.; Fitzpatrick, E.; Dhawan, A. Human hepatocyte transplantation for liver disease: current status and future perspectives. *Pediatr. Res.* **2018**, *83* (1), 232−240.

(18) Gritsay, D. V.; Lebedinskiy, A. S.; Ochenashko, O. V.; Petrenko, Y. A.; Volina, V. V.; Volkova, N. A.; Petrenko, A. Y. Liver Structure in Rats with Experimental Hepatic Failure Following Implantation of Macroporous Carrier Seeded with Cryopreserved Fetal Liver Cells. *Probl. Cryobiol. Cryomed.* **2014**, *24* (4), 292−301.

(19) Sudo, R. Multiscale tissue engineering for liver reconstruction. *Organogenesis* **2014**, *10* (2), 216−224.

(20) Fausto, N. Liver regeneration. *Journal of Hepatology* **2000**, *32* (suppl. 1), 19−31.

(21) Hammond, J. S.; Gilbert, T. W.; Howard, D.; Zaitoun, A.; Michalopoulos, G.; Shakesheff, K. M.; Beckingham, I. J.; Badylak, S. F. Scaffolds containing growth factors and extracellular matrix induce hepatocyte proliferation and cell migration in normal and regenerating rat liver. *Journal of Hepatology* **2011**, *54*, 279−287.

(22) Cho, C. S.; Seo, S. J.; Park, I. K.; Kim, S. H.; Kim, T. H.; Hoshiba, T.; Harada, I.; Akaike, T. Galactose-carrying polymers as extracellular matrices for liver tissue engineering. *Biomaterials.* **2006**, *27*, 576−585.

(23) Huang, G.; Li, F.; Zhao, X.; Ma, Y.; Li, Y.; Lin, M.; Jin, G.; Lu, T. J.; Genin, G. M.; Xu, F. Functional and Biomimetic Materials for Engineering of the Three-Dimensional Cell Microenvironment. *Chem. Rev.* **2017**, *117*, 12764−12850.

(24) Liu, C.; Xia, Z.; Czernuszka, J. T. Design and development of three-dimensional scaffold for tissue engineering. *Trans. Chem. E, Part A, Chemical Engineering Research and Design* **2007**, *85* (A7), 1051−1064.

(25) Bhandari, R. N.; Riccalton, L. A.; Lewis, A. L.; Fry, J. R.; Hammond, A. H.; Tendler, S. J.B.; Shakesheff, K. M. Liver tissue engineering: a role for co-culture systems in modifying hepatocyte function and viability. *Tissue Eng.* **2001**, *7*, 345−357.

(26) Christoffersson, J.; Aronsson, C.; Jury, M.; Selegård, R.; Aili, D.; Mandenius, C.-F. Fabrication of modular hyaluronan-PEG hydrogels to

support 3D cultures of hepatocytes in a perfused liver-on-a-chip device. *Biofabrication* **2019**, *11*, 015013.
(27) Xing, Q.; Qian, Z.; Jia, W.; Ghosh, A.; Tahtinen, M.; Zhao, F. Natural Extracellular Matrix for Cellular and Tissue Biomanufacturing. *ACS Biomater. Sci. Eng.* **2017**, *3*, 1462−1476.
(28) Stevens, K. R.; Scull, M. A.; Ramanan, V.; Fortin, L.; Chaturvedi, R. R.; Knouse, K. A.; Xiao, S. W.; Fung, C.; Mirabella, T. In situ expansion of engineered human liver tissue in a mouse model of chronic liver disease. *Sci. Transl. Med.* **2017**, *9*, 5505.
(29) Ijima, H.; Nakamura, S.; Bual, R. P.; Yoshida, K. Liver-specific extracellular matrix hydrogel promotes liver-specific functions of hepatocytes in vitro and survival of transplanted hepatocytes in vivo. *J. Biosci. Bioeng.* **2019**, *128*, 365−72.
(30) Pedraz, J. L., Orive, G., Eds. *Therapeutic Applications of Cell Microencapsulation*; Springer: New York, 2010; Vol. *670*, pp 92−103; DOI: 10.1007/978-1-4419-5786-3_9.
(31) Farina, M.; Alexander, J. F.; Thekkedath, U.; Ferrari, M.; Grattoni, A. Cell encapsulation: Overcoming barriers in cell transplantation in diabetes and beyond. *Adv. Drug Delivery Rev.* **2019**, *139*, 92−115.
(32) Dong, H.; Fahmy, T. M.; Metcalfe, S. M.; Morton, S. L.; Dong, X.; Inverardi, L.; Adams, D. B.; Gao, W.; Metcalfe, H. W. Immuno-Isolation of Pancreatic Islet Allografts Using Pegylated Nanotherapy Leads to Long-Term Normoglycemia in Full MHC Mismatch Recipient Mice. *PLoS One* **2012**, *7* (12), e50265.
(33) Omami, M.; McGarrigle, J. J.; Reedy, M.; Isa, D.; Ghani, S.; Marchese, E.; Bochenek, M. A.; Longi, M.; Xing, Y.; Joshi, I.; Wang, Y.; Oberholzer, J. Islet Microencapsulation: Strategies and Clinical Status in Diabetes. *Curr. Diab. Rep.* **2017**, *17*, 47.
(34) Ullah, S.; Chen, X. Fabrication, applications and challenges of natural biomaterials in tissue engineering. *Appl. Mater. Today* **2020**, *20*, 100656.
(35) Zarrintaj, P.; Manouchehri, S.; Ahmadi, Z.; Saeb, M. R.; Urbanskad, A. M.; Kaplan, D. L.; Mozafari, M. Agarose-based biomaterials for tissue engineering. *Carbohydr. Polym.* **2018**, *187*, 66−84.
(36) Yao, Q.; Zheng, Y.-W.; Lan, Q.-H.; Kou, L.; Xu, H.; Zhao, Y.-Z. Recent development and biomedical applications of decellularized extracellular matrix biomaterials. *Mater. Sci. Eng., C* **2019**, *104*, 109942.
(37) Mabrouk, M.; Beherei, H. H.; Das, D. B. Recent progress in the fabrication techniques of 3D scaffolds for tissue engineering. *Mater. Sci. Eng., C* **2020**, *110*, 110716.
(38) Legallais, C.; Kim, D.; Mihaila, S. M.; Mihajlovic, M.; Figliuzzi, M.; Bonandrini, B.; Salerno, S.; Yousef Yengej, F. A.; Rookmaaker, M. B.; Sanchez Romero, N.; Sainz-Arnal, P.; Pereira, U.; Pasqua, M.; Gerritsen, K. G. F.; Verhaar, M. C.; Remuzzi, A.; Baptista, P. M.; De Bartolo, L.; Masereeuw, R.; Stamatialis, D. Bioengineering organs for blood detoxification: artificial, bioartificial and tissue engineered kidney and liver. *Adv. Healthcare Mater.* **2018**, *7* (21), 1800430.
(39) Mazza, G.; Al-Akkad, W.; Rombouts, K.; Pinzani, M. Liver Tissue Engineering: From Implantable Tissue to Whole Organ Engineering. *Hepatology Communications* **2018**, *2*, 131−141.
(40) Agarwal, T.; Subramanian, B.; Maiti, T. K. Liver Tissue Engineering: Challenges and Opportunities. *ACS Biomater. Sci. Eng.* **2019**, *5*, 4167−4182A.
(41) Kokorev, O. V.; Khodorenko, V. N.; Baigonakova, G. A.; Marchenko, E. S.; Yasenchuk, Yu. F.; Gunther, V. E.; Anikeev, S. G.; Barashkova, G. A. Metal-glass-ceramic phases on the surface of porous NiTi-based SHS-material for carriers of cells. *Russ. Phys. J.* **2019**, *61* (9), 1734−1740.
(42) Yasenchuk, Y.; Marchenko, E.; Gunther, V.; Radkevich, A.; Kokorev, O.; Gunther, S.; Baigonakova, G.; Hodorenko, V.; Chekalkin, T.; Kang, J.; Weiss, S.; Obrosov, A. Biocompatibility and Clinical Application of Porous TiNi Alloys Made by Self-Propagating High-Temperature Synthesis (SHS). *Materials* **2019**, *12* (15), 2405.
(43) Yuan, B.; Zhu, M.; Chung, C. Y. Biomedical Porous Shape Memory Alloys for Hard-Tissue Replacement Materials. *Materials* **2018**, *11*, 1716.
(44) Elahinia, M. H.; Hashemi, M.; Tabesh, M.; Bhaduri, S. B. Manufacturing and processing of NiTi implants: A review. *Prog. Mater. Sci.* **2012**, *57*, 911−946.
(45) Kokorev, O. V.; Hodorenko, V. N.; Chekalkin, T. L.; Kim, J.-S.; Kang, S.-B.; Ts. Dambaev, G.; Gunther, V. E. In vitro and in vivo evaluation of porous TiNi-based alloy as a scaffold for cell tissue engineering. *Artificial Cells, Nanomedicine, and Biotechnology* **2016**, *44*, 704−709.
(46) Gunter, V. E.; Ts. Dambaev, G.; Kokorev, O. V. Permeable nickel titanium incubator. Patent No. 2638819 RF, MPK A61L 27/56 (200601) No. 2016127151; Applied 2016-05-06; published 2017-12-15, Bul. 35.
(47) Shimizu, K.; Ito, A.; Honda, H. Enhanced cell-seeding into 3D porous scaffolds by use of magnetite nanoparticles. *J. Biomed. Mater. Res. Part B Appl. Biomater.* **2006**, *77B*, 265−272.
(48) Fan, J.; Jia, X.; Huang, Y.; Fu, B. M.; Fan, Y. Greater scaffold permeability promotes growth of osteoblastic cells in a perfused bioreactor. *J. Tissue Eng. Regen. Med.* **2015**, *9*, E210−E218.
(49) Chung, E. J.; Ju, H. W.; Park, H. J.; Park, C. H. Three-layered scaffolds for artificial esophagus using poly(-caprolactone) nanofibers and silk fibroin: An experimental study in a rat model. *J. Biomed. Mater. Res. Part A* **2015**, *103*, 2057−2065.
(50) Tamjid, E.; Simchi, A.; Dunlop, J. W.; Fratzl, P.; Bagheri, R.; Vossoughi, M. Tissue growth into three-dimensional composite scaffolds with controlled micro-features and nanotopographical surfaces. *J. Biomed. Mater. Res. Part A* **2013**, *101*, 2796−2807.
(51) Gunter, S. V.; Marchenko, E. S.; Yasenchuk, Y. F.; Baigonakova, G. A.; Volinsky, A. A. Portable universal tensile testing machine for studying mechanical properties of superelastic biomaterials. *Engineering Research Express* **2021**, *3* (4), 045055.
(52) Baigonakova, G. A.; Marchenko, E. S.; Kovaleva, M. A.; Chudinova, E. A.; Volinsky, A. A.; Zhang, Y. Thickness effects on the martensite transformations and mechanical properties of nanocrystalline NiTi wires. *Nanomaterials* **2022**, *12* (42), 4442.
(53) Tamjid, E.; Simchi, A.; Dunlop, J. W.; Fratzl, P.; Bagheri, R.; Vossoughi, M. Tissue growth into three-dimensional composite scaffolds with controlled micro-features and nanotopographical surfaces. *J. Biomed. Mater. Res. Part A* **2013**, *101*, 2796−2807.
(54) *Directive 2010/63/EU of the European Parliament and of the Council of 22 September 2010 on the protection of animals used for scientific purposes*; 2010; https://eur-lex.europa.eu/LexUriServ/LexUriServ.do?uri=OJ:L:2010:276:0033:0079:EN:PDF.
(55) Shen, L.; Hillebrand, A.; Wang, D.; Liu, M. Isolation and primary culture of rat hepatic cells. *J. Vis. Exp.* **2012**, *64*, 1 DOI: 10.3791/3917.
(56) Mueller, S.; Sandrin, L. Liver stiffness: A novel parameter for the diagnosis of liver disease. *Hepat. Med.Evid. Res.* **2010**, *2*, 49−67.
(57) Ali, S.; Khan, M. R.; Shah, S. A.; Batool, R.; Maryam, S.; Majid, M.; Zahra, Z. Protective aptitude of Periploca hydaspidis Falc against CCl_4 induced hepatotoxicity in experimental rats. *Biomedicine & Pharmacotherapy* **2018**, *105*, 1117−1132.
(58) Petrenko, Y. A.; Ivanov, R. V.; Petrenko, A. Yu; Lozinsky, V. I. Coupling of gelatin to inner surfaces of pore walls in spongy alginate-based scaffolds facilitates the adhesion, growth and differentiation of human bone marrow mesenchymal stromal cells. *J. Mater. Sci: Mater. Med.* **2011**, *22*, 1529−1540.
(59) Bhatia, S. N.; Underhill, G. N.; Zaret, K. S.; Fox, I. J. Cell and tissue engineering for liver disease. *Sci. Transl. Med.* **2014**, *6* (245), 245sr2.
(60) Dhawan, A.; Puppi, J.; Hughes, R. D.; Mitry, R. R. Human hepatocyte transplantation: current experience and future challenges. *Nat. Rev. Gastroenterol. Hepatol.* **2010**, *7*, 288−298.
(61) Gunther, V.; Radkevich, A.; Kang, S. B.; Chekalkin, T.; Marchenko, E.; Gunther, S.; Pulikov, A.; Sinuk, I.; Kaunietis, S.; Podgorniy, V.; Chang, M. J.; Kang, J. H. Study of the knitted TiNi mesh graft in a rabbit cranioplasty model. *Biomedical Physics Engineering Express* **2019**, *5* (2), 027005.
(62) Shtin, V. I.; Novikov, V. A.; Chekalkin, T. L.; Gunther, V.; Marchenko, E.; Choynzonov, E.; Kang, S. B.; Chang, M. J.; Kang, J. H.;

Obrosov, A. Repair of orbital post-traumatic wall defects by custom-made TiNi mesh endografts. *J. Funct. Biomater.* **2019**, *10* (3), 27.

https://doi.org/10.1021/acsbiomaterials.2c01268
ACS Biomater. Sci. Eng. 2023, 9, 1558−1569